Renormalization-group approach to the Manna sandpile

Chai-Yu Lin
Department of Physics, National Chung Cheng University, Chia-Yi 62102, Taiwan and National Center for Theoretical Sciences at Taipei, Physics Division, National Taiwan University, Taipei 10617, Taiwan

(Received 29 July 2009; revised manuscript received 10 January 2010; published 4 February 2010)

In this paper a renormalization group (RG) scheme for the q-state Manna model is proposed based on the stochastic characteristic and the similarity of topplings at different scales. A full enumeration of the RG evolution events inside a 2×2 RG cell for $q=2$, 3, and 4 was carried out. A fixed point analysis shows that the resulting height probabilities are very close to the results obtained by the numerical simulations. The calculations of the toppling number exponent τ and the dynamical exponent z are also provided. It was found that the RG values of τ and z for $q=4$ are very close to the simulation values.

DOI: 10.1103/PhysRevE.81.021112 PACS number(s): 05.50.+q, 45.70.Cc, 05.65.+b, 05.70.Jk

I. INTRODUCTION

The concept of self-organized criticality (SOC) [1,2] provides a possible pathway for explaining the power-law behavior in many natural phenomena. The language of the sandpile avalanche is normally used to introduce SOC. The Bak-Tang-Wiesenfeld (BTW) [1] and Manna [3] models are prototypes for deterministic and stochastic sandpiles, respectively. In addition to the enormous body of numerical data, e.g., Refs. [4–6], and a few exact solutions, e.g., Refs. [7,8], the renormalization group (RG) approach has the potential to advance the understanding of the sandpile.

In 1994, Pietronero, Vespignani, and Zapperi (PVZ) [9] proposed the so-called dynamically driven RG scheme for sandpiles. In their study the RG equation was established by counting the relaxation events in the map between the 2×2 RG cells of different scales. Subsequently, Ivashkevich [10] furnished the BTW RG scheme after considerable refinement of the PVZ RG scheme. Later, the dynamically driven RG was applied to the directed sandpile [11]. More recently, Lin *et al.* [12] proposed a Monte Carlo procedure instead of an exact enumeration for relaxation events.

Based on the PVZ RG scheme, the BTW and Manna models are in the same universality class. However, some numerical evidence has shown that the BTW model follows multifractal scaling, e.g., Ref. [13], while the Manna model exhibits simple scaling, e.g., Refs. [4,6]. Therefore, it is necessary to develop a RG scheme for the Manna model. Based on the RG framework provided by PVZ and Ivashkevich, we propose a RG scheme that highlights the stochastic characteristic of the Manna model. Our proposed RG scheme leads to the resulting height probabilities, the toppling number exponent, and the dynamical exponent, which are consistent with the corresponding results obtained from the numerical simulations.

The version of the Manna model used in this paper is established on a square lattice $\mathcal{L}_0$ paved with zero squares (square domains of size $2^\lambda\times2^\lambda$ for $\lambda=0$). Some grains are distributed over $\mathcal{L}_0$. The number of grains located in one zero square $i^{(0)}$ is $h_{i^{(0)}}$ which is called the height. The value of q is the sandpile toppling threshold. A zero square $i^{(0)}$ with a height larger than or equal to q ($h_{i^{(0)}}\geq q$) is called an unstable zero square. Otherwise, it is called a stable zero square. An unstable square $i^{(0)}$ will topple. The toppling rules are (i) to decrease the height of the toppling zero square $i^{(0)}$ by q and (ii) to operate the increasing procedure q times. Increasing the value of the height of a randomly chosen nearest neighbor (NN) of the toppling zero square $i^{(0)}$ by 1 is called the increasing procedure. The toppling rule can be formulated as

$$h_{i^{(0)}}\rightarrow h_{i^{(0)}}-q,$$

$$h_{\mathrm{NN}_k(i^{(0)})}\rightarrow h_{\mathrm{NN}_k(i^{(0)})}+1 \quad \text{for } k=1,2,\ldots,q, \tag{1}$$

where $\mathrm{NN}_k(i^{(0)})$ is a randomly chosen NN of the zero square $i^{(0)}$ from the kth operation of the increasing procedure.

Initially, all zero squares are stable. We trigger the sandpile by adding one grain to one randomly chosen zero square $i^{(0)}=I$. If the zero square I is unstable, a series of topplings will occur as per Eq. (1). The corresponding evolution is called an avalanche. When the evolution stops (all zero squares are stable), we measure the toppling number s. We repeatedly trigger the sandpile system and record s for every avalanche. The probability distribution of the toppling number $D(s)$ is expected to be the power-law form $D(s)\sim s^{-\tau}$ or the finite-size scaling form $D(s)=s^{-\tau}\Theta(s/L^\gamma)$, where τ is the toppling number exponent, Θ is a scaling function, L is the lattice size, and γ is the cutoff exponent of the toppling number. Figure 1 shows the probability distribution $D(s)$ for the q-state Manna model on a $L\times L$ square lattice where $(q,L)=(2,128)$, (2,256), (2,512), (3,512), and (4,512). For $L=512$, we found that the curves of $D(s)$ for $q=2$, 3, and 4 are nearly identical. Thus, we expect that $D(s)$ is independent of q. In the inset of Fig. 1, $s^\tau D(s)$ as a function of s/L^γ is shown. It should be noted that we used $\tau=1.27$ and $\gamma=2.73$ which were obtained from extensive simulations of $q=2$ [5]. This inset exhibits the existence of scaling function $\Theta(s/L^\gamma)$. In short, Fig. 1 shows that the q-state Manna model for different q shares the same universality class [6], i.e., the values of τ and γ are the same for different q.

II. COARSE-GRAINING PROCEDURE AND THE RG PARAMETERS

Let us take a square lattice $\mathcal{L}_\lambda$ paved with the λ squares (the square domains of size $2^\lambda\times2^\lambda$). Examples are shown in

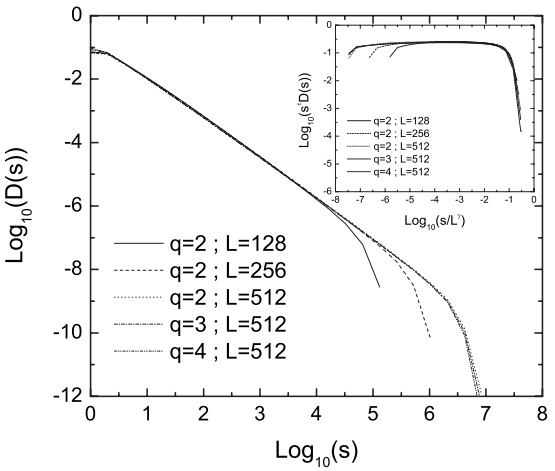

FIG. 1. Probability distribution $D(s)$ as a function of s for $q=2$, 3, and 4 on a $L\times L$ square lattice. (inset) $s^{\tau}D(s)$ as a function of s/L^{γ}, where $\tau=1.27$ and $\gamma=2.73$.

Figs. 2(a)–2(d) for $\lambda=0$, 1, 2, and 3, respectively. Since the sandpile described by zero squares on $\mathcal{L}_0$ is presented in Sec. I, it is worthwhile to create the sandpile described by λ squares on $\mathcal{L}_\lambda$, i.e., the coarse-grained sandpile.

For an avalanche, if a zero square $i^{(0)}$ has ever experienced an unstable status and then has toppled through Eq. (1), then this zero square that transferred grains to its NNs is called a dynamic zero square. Otherwise, it is called a stationary zero square. An example is shown in Fig. 2(a). A $(\lambda+1)$ square on $\mathcal{L}_{\lambda+1}$ is equivalent to a 2×2 RG cell on $\mathcal{L}_\lambda$ consisting of four λ squares. PVZ provided a coarse-graining procedure [9] to establish the dynamic $(\lambda+1)$ squares on $\mathcal{L}_{\lambda+1}$ from the dynamic λ squares on $\mathcal{L}_\lambda$. The procedure is described as follows. If the dynamic λ squares located inside a $(\lambda+1)$ square span this $(\lambda+1)$ square from top to bottom or from left to right, this $(\lambda+1)$ square is referred to as a dynamic $(\lambda+1)$ square. Otherwise, it is called a stationary $(\lambda+1)$ square. Consider the example shown in Fig. 2(a) with

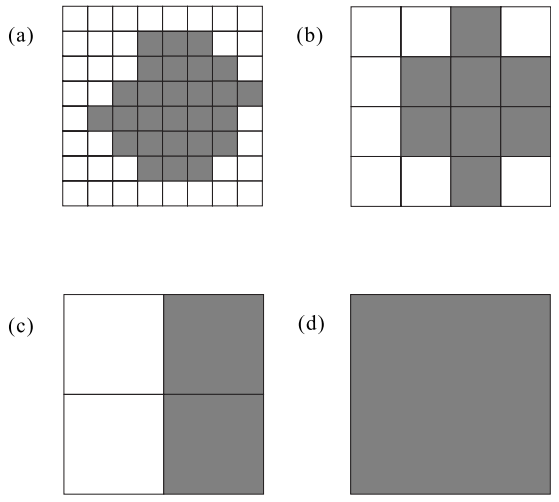

FIG. 2. The coarse-graining procedure for an avalanche. The λ square filled in gray is the dynamic λ square: (a) $\lambda=0$, (b) $\lambda=1$, (c) $\lambda=2$, and (d) $\lambda=3$.

the dynamic and stationary zero squares. If we run the coarse-graining procedure for $\lambda=0$, then we obtain the dynamic and stationary one squares [see Fig. 2(b)]. If we then iterate this procedure for $\lambda=1$ and $\lambda=2$, we obtain the dynamic and stationary squares of every stage [see Figs. 2(c) and 2(d)].

For the sandpile on $\mathcal{L}_\lambda$, the dynamic λ squares are now well defined. However, the definitions of the unstable status and the toppling rule are still absent. To complete the task, we define a non-negative integer $h_{i^{(\lambda)}}$ as the coarse-grained height of the λ square $i^{(\lambda)}$. Like the sandpile on $\mathcal{L}_0$, if $h_{i^{(\lambda)}}\geq q$ $(0\leq h_{i^{(\lambda)}}<q)$, then the λ square $i^{(\lambda)}$ is called an unstable (a stable) λ square. Unlike an unstable zero square which topples through one single toppling rule [i.e., Eq. (1)], an unstable λ square $i^{(\lambda)}$ may topple through the RG toppling rules $T_1, T_2, \ldots,$ or T_q. The probability of picking one specific T_α is $p_\alpha^{(\lambda)}$, where $\Sigma_{\alpha=1}^{q} p_\alpha^{(\lambda)}=1$. We formulate T_α as

$$T_\alpha=\begin{cases} h_{i^{(\lambda)}}\rightarrow h_{i^{(\lambda)}}-\alpha \\ h_{\mathrm{NN}_k(i^{(\lambda)})}\rightarrow h_{\mathrm{NN}_k(i^{(\lambda)})}+1 \quad \text{for } k=1,2,\ldots,\alpha, \end{cases} \tag{2}$$

where the λ square $\mathrm{NN}_k(i^{(\lambda)})$ is a randomly chosen NN of the λ square $i^{(\lambda)}$ from the kth operation of the increasing procedure. In Eq. (2), $h_{i^{(\lambda)}}\rightarrow h_{i^{(\lambda)}}-\alpha$ refers to the RG scheme of PVZ [9], $h_{\mathrm{NN}_k(i^{(\lambda)})}\rightarrow h_{\mathrm{NN}_k(i^{(\lambda)})}+1$ performs the stochastic feature of the Manna model, and $k=1,2,\ldots,\alpha$ means the conservation of the coarse-grained heights of the λ square $i^{(\lambda)}$ and its NNs. We then define the λ grain such that $h_{i^{(\lambda)}}$ is the number of λ grains located in one λ square $i^{(\lambda)}$. Equation (2) can then be written such that the λ square $i^{(\lambda)}$ releases α λ grains and that the λ square $\mathrm{NN}_k(i^{(\lambda)})$ receives one λ grain at the kth operation of the increasing procedure. Therefore, for an avalanche, if a λ square $i^{(\lambda)}$ has experienced an unstable status and has then toppled through Eq. (2), then this λ square will transfer λ grains to its NNs and is called a dynamic λ square.

We define the first set of RG parameters as

$$\vec{p}^{(\lambda)}=(p_1^{(\lambda)},p_2^{(\lambda)},\ldots,p_q^{(\lambda)}). \tag{3}$$

The sandpile on $\mathcal{L}_0$ corresponds to $\vec{p}^{(0)}=(0,\cdots,1)$ where $T_1,\cdots,T_{q-1}$ are forbidden (i.e., $p_\alpha^{(0)}=0$ for $\alpha<q$) and only T_q is allowable (i.e., $p_\alpha^{(0)}=1$ for $\alpha=q$). The purpose of this paper is to determine the value of $\vec{p}^{(\lambda)}$ for $\lambda\geq 1$. We then further classify T_α into $T_{\alpha,d_1\ldots d_\alpha}$, where d_k=E, N, W, or S, which correspond to the eastern NN (E-NN), northern NN, western NN, or southern NN chosen at the kth operation for $h_{\mathrm{NN}_k(i^{(\lambda)})}\rightarrow h_{\mathrm{NN}_k(i^{(\lambda)})}+1$ of Eq. (2). There are 4^α versions for one specific T_α, e.g., T_1 can be $T_{1,\mathrm{E}}$, $T_{1,\mathrm{N}}$, $T_{1,\mathrm{W}}$, or $T_{1,\mathrm{S}}$ (four versions) and T_2 can be $T_{2,\mathrm{EE}}$, $T_{2,\mathrm{EN}},\ldots,$ or $T_{2,\mathrm{SS}}$ (4^2 versions). The probability of occurrence of one specific $T_{\alpha,d_1\ldots d_\alpha}$ is $(1/4^\alpha)p_\alpha^{(\lambda)}$.

Let us consider that the topplings due to one triggering on $\mathcal{L}_0$ have stopped and that the system has not experienced the next triggering. All zero squares are stable. After running the coarse-graining procedure, this situation corresponds to the fact that all λ squares on $\mathcal{L}_\lambda$ are stable, i.e., $0\leq h_{i^{(\lambda)}}\leq q-1$

for all $i^{(\lambda)}$. In this case, we consider that $n_\beta^{(\lambda)}$ is the probability of $h_{i^{(\lambda)}}=\beta$. We define the second set of RG parameters as

$$\vec{n}^{(\lambda)} = (n_0^{(\lambda)}, n_1^{(\lambda)}, \ldots, n_{q-1}^{(\lambda)}), \tag{4}$$

where $\Sigma_{\beta=0}^{q-1} n_\beta^{(\lambda)}=1$.

By extending the idea of Ivashkevich [10], the relationship between $\vec{n}^{(\lambda)}$ and $\vec{p}^{(\lambda)}$ can be expressed as

$$dn_\beta^{(\lambda)}/dt \sim n_{\beta-1}^{(\lambda)} + n_{q-1}^{(\lambda)} p_{q-\beta}^{(\lambda)} - n_\beta^{(\lambda)}, \tag{5}$$

where $n_{-1}^{(\lambda)}=0$. Equation (5) describes the height of a stable λ square receiving one λ grain. The rate of change of $n_\beta^{(\lambda)}$ [i.e., $dn_\beta^{(\lambda)}/dt$ in Eq. (5)] consists of items (i)–(iii) in the right-hand side of Eq. (5). Item (i) describes that the original height is $\beta-1$. Finally the height becomes β after receiving one λ grain. Item (ii) describes that the original height is $q-1$. After receiving one λ grain, the height becomes q. Then, this λ square topples and employs toppling rule $T_{q-\beta}$. Finally, the height of this λ square is also β. Item (iii) describes that the original height is β. The final height becomes $\beta+1$ after receiving one λ grain. By putting the steady-state assumption $dn_\beta^{(\lambda)}/dt=0$ into Eq. (5), the relationship between $\vec{n}^{(\lambda)}$ and $\vec{p}^{(\lambda)}$ becomes

$$n_\beta^{(\lambda)} = \sum_{\alpha=q,-1}^{q-\beta} p_\alpha^{(\lambda)} \Big/ \sum_{\alpha=1}^{q} \alpha p_\alpha^{(\lambda)}. \tag{6}$$

III. PROBABILITY OF EVOLUTIONS INSIDE A RG CELL

A 2×2 RG cell on $\mathcal{L}_\lambda$ consists of four λ squares labeled by $i^{(\lambda)}$=left top (LT), left bottom (LB), right top (RT), and right bottom (RB). The positions of these four λ squares marked by △ (LT), ◁ (LB), ▷ (RT), and ▽ (RB) are shown in one configuration of Fig. 3(a.1). Set $\Phi=\{\mathrm{LT},\mathrm{LB},\mathrm{RT},\mathrm{RB}\}$. Next we consider the evolutions of the RG cell with the height configuration $[h_{\mathrm{LT}}(t),h_{\mathrm{LB}}(t),h_{\mathrm{RT}}(t),h_{\mathrm{RB}}(t)]$ at the tth evolution step. At $t=0$, the heights are all stable, i.e., $0\le h_{i^{(\lambda)}}(0)\le q-1$ for all $i^{(\lambda)}\in\Phi$. A λ square $i^{(\lambda)}\in\Phi$ where $h_{i^{(\lambda)}}(0)=q-1$ is called a critical λ square and is denoted as J. The number of critical λ squares in the RG cell is M.

Consider that the sandpile evolution of the RG cell is initialized by receiving one λ grain from outside of the cell. Since we are interested in that an RG cell on $\mathcal{L}_\lambda$ can generate dynamic λ squares, the requirements (I) about $[h_{\mathrm{LT}}(0),h_{\mathrm{LB}}(0),h_{\mathrm{RT}}(0),h_{\mathrm{RB}}(0)]$ and (II) about J must be fulfilled and described in the following sentences.

(I) It states that every height configuration at $t=0$ must possess critical λ squares, i.e., $M\ge1$. One $[h_{\mathrm{LT}}(t),h_{\mathrm{LB}}(t),h_{\mathrm{RT}}(t),h_{\mathrm{RB}}(t)]$ at $t=0$ that satisfies requirement (I) is denoted as $H(t)$. In Fig. 3(a.1), for $q=2$, all $H(0)$ are categorized into five types. Each type possesses A kinds of configurations which are invariant to each other through rotating $k'\pi/2$ radians, where k' is an integer. In Fig. 3(a.2), the representative $H(0)$ chosen from Fig. 3(a.1) are listed according to each type.

(II) It states that one λ grain is added to one of these critical λ squares. Thus, a critical λ square J receives one λ grain from outside of the RG cell. Then, we have

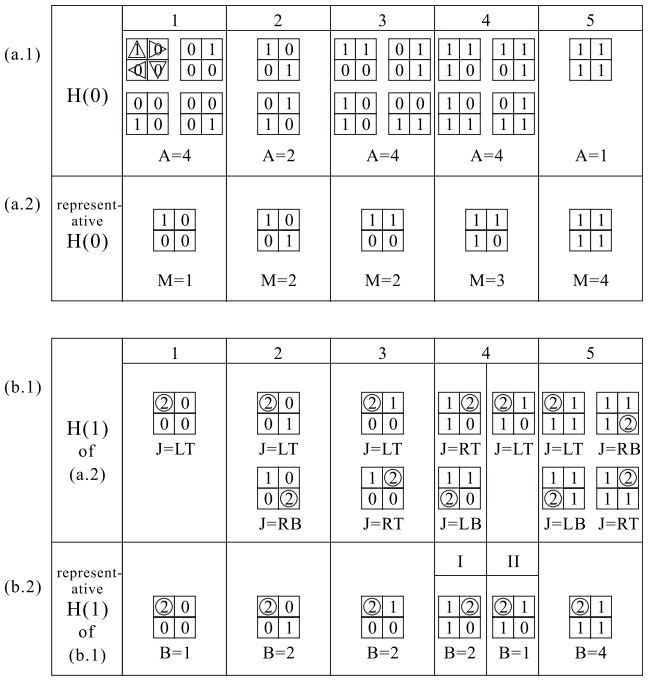

FIG. 3. The height of a square is printed inside the square. An unstable square is marked by ○. (a.1) All $H(0)$ are divided into five types where A is the number of copies for rotational invariance. The positions of the λ square LT (marked by △), the λ square LB (marked by ◁), the λ square RT (marked by ▷), and the λ square RB (marked by ▽) are shown in a configuration of type 1. (a.2) The representative $H(0)$ of each type where M is the number of the critical λ squares. (b.1) The 12 kinds of $H(1)$ generated from the representative $H(0)$ shown in (a.2). (b.2) The six kinds of $H(1)$ involving the RG calculation where B is the number of copies for symmetrical invariance.

$$h_{i^{(\lambda)}}(1) = h_{i^{(\lambda)}}(0) \quad \text{for } i^{(\lambda)} \neq J,$$

$$h_{i^{(\lambda)}}(1) = h_{i^{(\lambda)}}(0) + 1 = q \quad \text{for } i^{(\lambda)} = J. \tag{7}$$

Figure 3(b.1) shows all possible J and $H(1)$ evolving from the representative $H(0)$ in Fig. 3(a.2).

If requirements (I) and (II) do not hold [i.e., $h_{i^{(\lambda)}}(1)<q$ for all $i^{(\lambda)}\in\Phi$], the evolution stops at $t=1$ where none of λ squares LT, LB, RT, and RB are the dynamic λ square.

The probability of picking one specific $H(0)$ is

$$w[H(0)] = \prod_{i^{(\lambda)}\in\Phi} n_{h_{i^{(\lambda)}}(0)}. \tag{8}$$

Each configuration of Figs. 3(a.1) and 3(a.2) corresponds to the probabilities $n_0^3 n_1$ (type 1: $A=4$), $n_0^2 n_1^2$ (type 2: $A=2$), $n_0^2 n_1^2$ (type 3: $A=4$), $n_0 n_1^3$ (type 4: $A=4$), and n_1^4 (type 5: $A=1$). For a fixed $H(0)$, there are M choices for one specific J. Thus, the probability of picking one specific J is

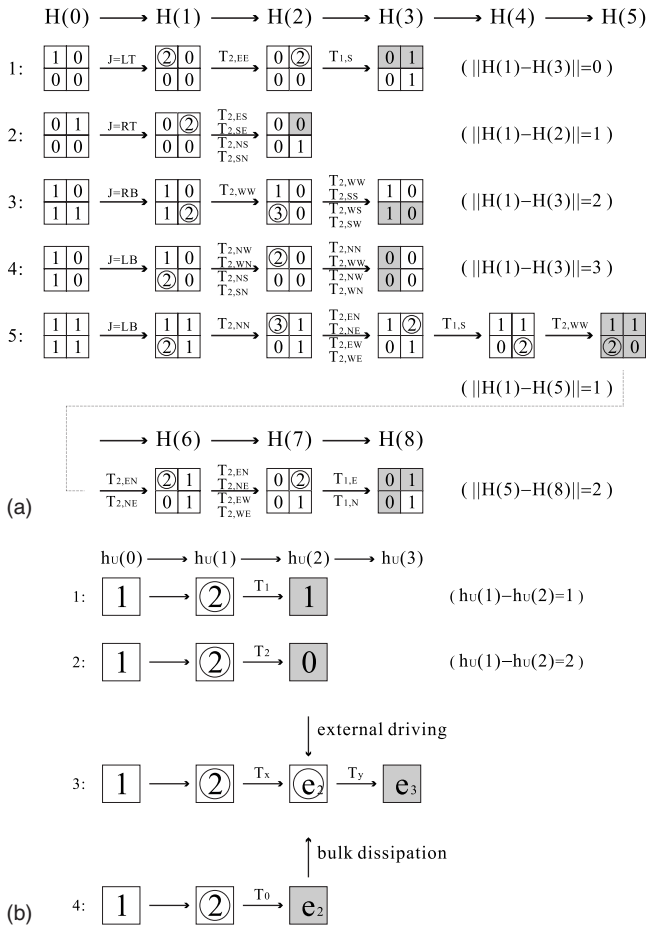

FIG. 4. (a) Details of the evolutions of $H(t)$ where the J and all possible $T_{\alpha,d_1\cdots d_\alpha}$ are shown together with the "→" of $H(t)\to H(t+1)$. An unstable square is marked by ○. All dynamic squares are filled in gray and shown in their final height configuration $H(t_f^{(\lambda)})$. Note that $t_f^{(\lambda)}=5$ if we use the freezing rule. (b) The evolution of $h_U(t)$. All dynamic squares are filled in gray and shown in their final height $h_U(t_f^{(\lambda+1)})$.

$$\Re[H(1)|H(0)]=\frac{1}{M}. \tag{9}$$

Consequently, the probability of the occurrence of one specific $H(1)$ is

$$w[H(1)]=\Re[H(1)|H(0)]w[H(0)], \tag{10}$$

where $w[H(1)]=\frac{1}{1}n_0^3n_1$ (type 1: $M=1$), $\frac{1}{2}n_0^2n_1^2$ (type 2: $M=2$), $\frac{1}{2}n_0^2n_1^2$ (type 3: $M=2$), $\frac{1}{3}n_0n_1^3$ (type 4: $M=3$), and $\frac{1}{4}n_1^4$ (type 5: $M=4$) for each configuration in Fig. 3(b.1).

The RG cell begins to relax. The height configuration evolving from $H(t)$ to $H(t+1)$ depends on Eq. (2) in parallel. Then, $H(1)$ and $\vec{H}(2,t_f^{(\lambda)})\equiv[H(2),H(3),\ldots,H(t_f)]$ record the toppling history, where $H(t_f^{(\lambda)})$ is the final height configuration. Figure 4(a) shows several evolutions from $H(0)$ to $H(t_f^{(\lambda)})$. If we define that

$$\|H(t')-H(t'')\|\equiv\sum_{i^{(\lambda)}\in\Phi}h_{i^{(\lambda)}}(t')-\sum_{i^{(\lambda)}\in\Phi}h_{i^{(\lambda)}}(t''), \tag{11}$$

$\|H(1)-H(t_f^{(\lambda)})\|$ with $t'=1$ and $t''=t_f^{(\lambda)}$ will represent the number of λ grains leaving the RG cell. Evolutions 1–4 of Fig. 4(a) show $\|H(1)-H(t_f^{(\lambda)})\|=0$, 1, 2, and 3, respectively. The probability of $H(t)$ evolving to $H(t+1)$ is $\Re[H(t+1)|H(t)]$ depending on the toppling rules of the toppled λ squares, e.g., $\Re[H(2)|H(1)]=\frac{1}{16}p_2^{(\lambda)}$ (the toppling rule is $T_{2,\mathrm{EE}}$) and $\Re[H(3)|H(2)]=\frac{1}{4}p_1^{(\lambda)}$ (the toppling rule is $T_{1,\mathrm{S}}$) in Fig. 4(a.1) and $\Re[H(2)|H(1)]=\frac{4}{16}p_2^{(\lambda)}$ (the toppling rule is $T_{2,\mathrm{ES}}$, $T_{2,\mathrm{SE}}$, $T_{2,\mathrm{NS}}$, or $T_{2,\mathrm{SN}}$) in Fig. 4(a.2). The toppling probability is

$$\Re[\vec{H}(2,t_f^{(\lambda)})|H(1)]=\prod_{t=1}^{t_f^{(\lambda)}-1}\Re[H(t+1)|H(t)]. \tag{12}$$

Examples in Figs. 4(a.1)–4(a.4) show that $\Re[\vec{H}(2,t_f^{(\lambda)})|H(1)]=[\frac{1}{16}p_2^{(\lambda)}][\frac{1}{4}p_1^{(\lambda)}]$, $[\frac{4}{16}p_2^{(\lambda)}]$, $[\frac{1}{16}p_2^{(\lambda)}][\frac{4}{16}p_2^{(\lambda)}]$, and $[\frac{4}{16}p_2^{(\lambda)}][\frac{4}{16}p_2^{(\lambda)}]$, respectively.

IV. RG TRANSFORMATION

A 2×2 RG cell with the height configuration $(h_{\mathrm{LT}},h_{\mathrm{LB}},h_{\mathrm{RT}},h_{\mathrm{RB}})$ on $\mathcal{L}_\lambda$ is considered as one $(\lambda+1)$ square $i^{(\lambda+1)}=U$ with height h_U on $\mathcal{L}_{(\lambda+1)}$. The evolution $H(0)\to H(1)\to\cdots\to\vec{H}(t_f^{(\lambda)})$ is considered as $h_U(0)\to h_U(1)\to h_U(2)\to\cdots\to h_U(t_f^{(\lambda+1)})$, where the $(\lambda+1)$ square U $[h_U(0)=q-1]$ receives one $(\lambda+1)$ grain from outside $[h_U(1)=q]$ and finally stops toppling at evolution time $t=t_f^{(\lambda+1)}$ $[h_U(t_f^{(\lambda+1)})<q]$. Examples are shown in Fig. 4(b). For an evolution, the number of the received coarse grains from outside is $\|H(1)-H(0)\|=1$ for the RG cell and $h_U(1)-h_U(0)=1$ for the $(\lambda+1)$ square U. The number of left coarse grains is $\|H(1)-H(t_f^{(\lambda)})\|$ for the RG cell and $h_U(1)-h_U(t_f^{(\lambda+1)})$ for the $(\lambda+1)$ square U.

The ratio of the number of received coarse grains to the number of left coarse grains is $\|H(1)-H(0)\|/\|H(1)-H(t_f^{(\lambda)})\|$ for the RG cell and $h_U(1)-h_U(0)/h_U(1)-h_U(t_f^{(\lambda+1)})$ for the $(\lambda+1)$ square U. To maintain the values of the above ratios, we build the mapping

$$h_U(1)-h_U(t_f^{(\lambda+1)})=\|H(1)-H(t_f^{(\lambda)})\|. \tag{13}$$

Following Eq. (13), the evolutions described by Figs. 4(a.2) and 4(a.3) correspond to the topplings described by Figs. 4(b.1) and 4(b.2), respectively.

Four extra transformation rules of the proposed RG scheme are as follows:

(1) Spanning rule. According to the coarse-graining procedure of PVZ, this RG transformation only accepts that the dynamic λ squares [filled in gray for the $H(t_f^{(\lambda)})$ in Fig. 4(a)] inside the RG cell span the cell from top to bottom or from left to right [9]. The evolutions that do not follow the spanning rule are excluded, e.g., Fig. 4(a.2).

(2) Freezing rule. The λ squares LT, LB, RT, or RB may experience the multiple topplings during the evolution $H(1)\to\cdots\to\vec{H}(t_f^{(\lambda)})$. An example is shown in Fig. 4(a.5) where the λ squares LT, LB, and RT topple twice. Then, we set that the corresponding $(\lambda+1)$ square U displays the mul-

tiple topplings during the evolution $h_U(1)\to h_U(2)\to\cdots\to h_U(t_f^{(\lambda+1)})$. Note that λ squares LB, LT, RT, and RB topple once during $H(1)\to\cdots\to H(5)$ and λ squares LB, LT, and RT topple once during $H(5)\to\cdots\to H(8)$. In order to maintain the toppling number of a RG square at the λth and (λ+1)th stages, it is reasonable to assume that $H(1)\to\cdots\to\vec{H}(5)$ [Fig. 4(a.5)] maps to $h_U(1)\to h_U(2)$ [Fig. 4(b.3)] and $H(5)\to\cdots\to\vec{H}(8)$ [Fig. 4(a.5)] maps to $h_U(2)\to h_U(3)$ [Fig. 4(b.3)]. In this case, $h_U(1)=2$ and $h_U(2)=e_2<2$ because the $(\lambda+1)$ square U topples through toppling rule T_x. Then, the $(\lambda+1)$ square U topples again through toppling rule T_y for $h_U(2)\to h_U(3)$, where $h_U(2)=e_2\geq 2$ and $h_U(3)=e_3<2$. Now a contradiction seems to occur for e_2 because $h_U(1)\to h_U(2)$ yields $e_2=2-x<2$ and $h_U(2)\to h_U(3)$ yields $e_2=e_3+y\geq 2$. This contradiction can be terminated if an external driving, providing extra $e_3+y-2+x$ $(\lambda+1)$ grains to the $(\lambda+1)$ square U at $t=2$, takes place. Thus, the probability of $h_U(2)\to h_U(3)$ is proportional to the probability of the external driving and is thus related to the driving rate. It has been known that the criticality of a sandpile system corresponds to the driving rate being zero [14–16]. Thus, to keep the criticality of the system, we set the probability of $h_U(2)\to h_U(3)$ being zero. That is, we must ignore $H(5)\to\cdots\to\vec{H}(8)$ in Fig. 4(a.5). To achieve this goal, we propose the freezing rule as follows. When a specific λ square topples once, this λ square cannot topple again regardless of its height. For example, the λ square LB in Fig. 4(a.5) is unstable at $t=5$. The λ square LB cannot topple again at $t=5$ because it is unstable at $t=1$. Thus, the evolution stops at $t=5$, i.e., $H(t_f^{(\lambda)})=H(5)$. At this time, $H(1)\to\cdots\to H(5)$ map to $h_U(1)\to h_U(2)$, where $h_U(t_f^{(\lambda+1)})=h_U(2)$. The freezing rule allows a λ square to topple only once on $\mathcal{L}_\lambda$ and makes Eq. (13) still workable. Therefore, Fig. 4(a.5) without $H(6)\to H(7)\to\vec{H}(8)$ is equivalent to Fig. 4(b.1) in this framework.

(3) Forbidding rule. There is no T_0 [12] in the proposed RG transformation. However, from Eq. (13), the $(\lambda+1)$ square U topples through $T_{h_U(1)-h_U(2)}=T_0$ as $\|H(1)-H(2)\|=0$. In such case, the proposed RG schemes do not treat the $(\lambda+1)$ square U as a dynamic $(\lambda+1)$ square. Thus we exclude the evolutions with $\|H(1)-H(2)\|=0$, e.g., Fig. 4(a.1). From another viewpoint, Fig. 4(a.1) describing $H(1)\to\cdots\to\vec{H}(3)$ will map to Fig. 4(b.4) describing $h_U(1)\to h_U(2)$, where $h_U(2)=2$ based on Eq. (13). However, $t_f^{(\lambda)}=2$ and $h_U(2)<2$ should hold. This means that a bulk dissipation happens and then some $(\lambda+1)$ grains are removed from the system at $t=2$. This bulk dissipation makes $h_U(2)<2$. The probability of dissipation is related to the dissipation rate. It has been known that the criticality of a sandpile system happens when the dissipation rate is zero [14–17]. Therefore, this makes it evident why we do not consider T_0.

(4) Adjusting rule. From Eq. (13), $\|H(1)-H(t_f^{(\lambda)})\|>q$ corresponds to $h_U(1)-h_U(2)>q$. However, in this scheme $h_U(1)-h_U(2)\leq q$. Equation (13) is then adjusted approximately to let $h_U(1)-h_U(2)=q$ if $\|H(1)-H(t_f^{(\lambda)})\|>q$, e.g., Fig. 4(a.4) corresponds to Fig. 4(b.2).

V. RG EQUATION

The evolution $H(1)\to\vec{H}(2,t_f^{(\lambda)})$ satisfying four extra transformation rules and mapping to $\alpha'=h_U(1)-h_U(2)$ is called an α' event, where

$$\alpha' = h_U(1)-h_U(2) = \begin{cases} \|H(1)-H(t_f^{(\lambda)})\| & \text{if } \|H(1)-H(t_f^{(\lambda)})\|\leq q \\ q & \text{if } \|H(1)-H(t_f^{(\lambda)})\|>q \end{cases} \tag{14}$$

is obtained from Eq. (13) and the adjusting rule. The corresponding $\vec{H}(2,t_f^{(\lambda)})$ of an α' event is denoted as $\vec{H}(2,t_f^{(\lambda)};\alpha')$. Then $\vec{H}(2,t_f^{(\lambda)};\alpha')$ of all α' events with one fixed $H(1)$ are collected into a set $\{\vec{H}(2,t_f^{(\lambda)};\alpha')|H(1)\to\vec{H}(2,t_f^{(\lambda)};\alpha')\}$. The total toppling probability of all α' events with one fixed $H(1)$ is

$$F_{\alpha'}[H(1)] = \sum_{\vec{H}(2,t_f^{(\lambda)})\in\{\vec{H}(2,t_f^{(\lambda)};\alpha')|H(1)\to\vec{H}(2,t_f^{(\lambda)};\alpha')\}} \Re[\vec{H}(2,t_f^{(\lambda)})|H(1)]. \tag{15}$$

For the two-state Manna model, $\alpha'=1$ or 2 (from $q=2$), $t_f^{(\lambda)}\geq 3$ (form the spanning rule), and $t_f^{(\lambda)}\leq 5$ (from the freezing rule).

Some α' events with a fixed $H(1)=(2,0,0,0)$ and $H(2)=(0,0,2,0)$ are plotted in Figs. 5(a) and 5(b) where $\|H(1)-H(t_f^{(\lambda)})\|=1$ and in Fig. 5(c) where $\|H(1)-H(t_f^{(\lambda)})\|=2$. The summation of heights for $H(1)$ is 2. For the case $\|H(1)-H(t_f^{(\lambda)})\|=1$ (i.e., $\alpha'=1$), the summation of heights for $H(t_f^{(\lambda)})$ must be 1 (i.e., there are three λ squares with their heights being 0 and one λ square with its height being 1). Figures 5(a.1)–5(a.3) show the details of the evolutions for $t_f^{(\lambda)}=3$. The corresponding probabilities are $\Re[H(t_f^{(\lambda)})|H(t_f^{(\lambda)}-1)]=\frac{2}{4}p_1^{(\lambda)}$, $\frac{4}{16}p_2^{(\lambda)}$, and $\frac{4}{16}p_2^{(\lambda)}$, respectively. Figure 5(b.1) with parameters $(e_1,e_2,e_3)=(0,0,1)$, (1,0,0), and (0,1,0) is used to represent Figs. 5(a.1)–5(a.3), respectively. Therefore, Fig. 5(b.1) corresponds to probability $\Re[H(t_f)|H(t_f^{(\lambda)}-1)]=\frac{2}{4}p_1^{(\lambda)}+\frac{8}{16}p_2^{(\lambda)}$ which is the summation from Figs. 5(a.1)–5(a.3). Similarly, Fig. 5(b.2) with $t_f^{(\lambda)}=4$ and Fig. 5(b.3) with $t_f^{(\lambda)}=5$ also correspond to probability $\Re[H(t_f)|H(t_f^{(\lambda)}-1)]=\frac{2}{4}p_1^{(\lambda)}+\frac{8}{16}p_2^{(\lambda)}$. Thus, Figs. 5(b.1)–5(b.3) correspond to $\Re[\vec{H}(2,t_f^{(\lambda)})|H(1)]=uv_1$ $(t_f=3)$, u^2v_1 $(t_f=4)$, and u^3v_1 $(t_f=5)$, respectively, where $u=\frac{1}{16}p_2^{(\lambda)}$ and $v_1=\frac{2}{4}p_1^{(\lambda)}+\frac{8}{16}p_2^{(\lambda)}$.

For the case $\|H(1)-H(t_f^{(\lambda)})\|=2$ (i.e., $\alpha'=2$), the summation of heights for $H(t_f^{(\lambda)})$ must be 0 (i.e., four λ squares possess a height of 0). Figures 5(c.1)–5(c.3) correspond to $\Re[H(t_f^{(\lambda)})|H(t_f^{(\lambda)}-1)]=\frac{4}{16}p_2^{(\lambda)}$. Thus, Figs. 5(c.1)–5(c.3) correspond to $\Re[\vec{H}(2,t_f^{(\lambda)})|H(1)]=uv_2$ $(t_f=3)$, u^2v_2 $(t_f^{(\lambda)}=4)$, and u^3v_2 $(t_f^{(\lambda)}=5)$, respectively, where $v_2=\frac{4}{16}p_2^{(\lambda)}$. For the case $\|H(1)-H(t_f^{(\lambda)})\|=3$ (i.e., $\alpha'=2$ from the adjusting rule), the summation of heights for $H(t_f^{(\lambda)})$ must be −1. This is not allowed.

For $H(1)=(2,0,0,0)$, all α' events with a fixed $H(2)=(0,0,2,0)$ are plotted in Figs. 5(b) and 5(c). However, $H(2)=(0,2,0,0)$ is also possible. An example is shown in Fig. 5(d) where $H(2)=(0,2,0,0)$. Figures 5(b.1) and 5(d) are symmetrical to each other and correspond to the same top-

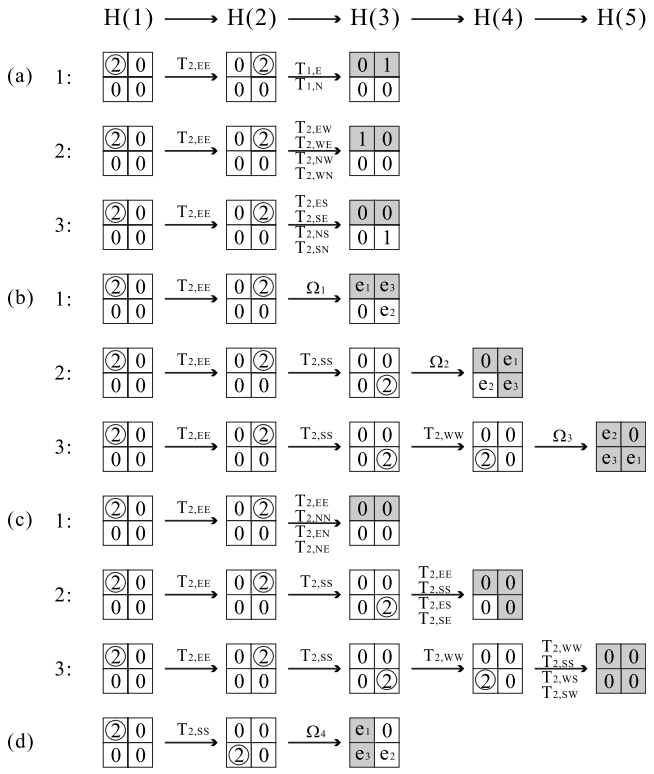

FIG. 5. The α' events for $q=2$. (a) Three one events with $H(1)=(2,0,0,0)$, $H(2)=(0,0,2,0)$, and $t_f=3$. (b) All one events with $H(1)=(2,0,0,0)$ and $H(2)=(0,0,2,0)$ where the parameters $(e_1,e_2,e_3)=(0,0,1)$, (1,0,0), and (0,1,0). The first event with $t_f=3$ is fully described by the events shown in (a.1)–(a.3) where $\Omega_1=T_{1,E}$, $T_{1,N}$ [from (a.1)], $T_{2,EW}$, $T_{2,WE}$, $T_{2,NW}$, $T_{2,WN}$ [from (a.2)], $T_{2,ES}$, $T_{2,SE}$, $T_{2,NS}$, and $T_{2,SN}$ [from (a.3)]. The second and third events correspond to $t_f=4$ and $t_f=5$, respectively, where Ω_2 and Ω_3 are similar to Ω_1. (c) All two events with $H(1)=(2,0,0,0)$ and $H(2)=(0,0,2,0)$. (d) An event with $H(1)=(2,0,0,0)$ and $H(2)=(0,2,0,0)$. This event and the event shown in (b.1) are symmetrical to each other and correspond to the same toppling probability.

pling probability. Each evolution in Figs. 5(b.1)–5(b.3) and 5(c.1)–5(c.3) has a corresponding symmetrical evolution with $H(2)=(0,2,0,0)$. Thus, for $H(1)=(2,0,0,0)$, we have $F_{\alpha'}[H(1)]=2(u+u^2+u^3)v_1$ for $\alpha'=1$ and $2(u+u^2+u^3)v_2$ for $\alpha'=2$. For general cases of $H(1)$, the enumeration of $F_{\alpha'}[H(1)]$ is rather laborious but straightforward.

From the obtained $H(1)$ and $F_{\alpha'}[H(1)]$ at the λth stage, the probability of the occurrence of $T_{\alpha'}$ on the $(\lambda+1)$th stage is

$$p_{\alpha'}^{(\lambda+1)}=\sum_{H(1)} w^{\#}[H(1)]F_{\alpha'}^{\#}[H(1)], \tag{16}$$

where $w[H(1)]$ is normalized to $w^{\#}[H(1)]=w[H(1)]/\{\Sigma_{H(1)}\, w[H(1)]\}$ and $F_{\alpha'}[H(1)]$ is normalized to $F_{\alpha'}^{\#}[H(1)]=F_{\alpha'}[H(1)]/\{\Sigma_{\alpha''=1}^{q} F_{\alpha''}[H(1)]\}$. Thus, we have $\Sigma_{\alpha'=1}^{q} p_{\alpha'}^{(\lambda+1)}=1$. Equation (16) is the RG equation describing the relationship between $p_{\alpha'}^{(\lambda+1)}$ for a specific α' and $p_{\alpha}^{(\lambda)}$ for $\alpha=1,\ldots,q$.

For $q=2$, the sum of AM for all types in Fig. 3 is 32. Thus, there are 32 kinds of $H(1)$ for calculating Eq. (16). In Fig. 3(b.1), there are M kinds of $H(1)$ for each type listed in Fig. 3(a.2). Each $H(1)$ leads to A kinds of copies with rotational invariance. Please note that the $w[H(1)]$ and $F_{\alpha'}[H(1)]$ are the same for the copies with rotational invariance. The sum of M over all types is 12. Therefore, to calculate Eq. (16), it is enough to use the 12 kinds of $H(1)$ shown in Fig. 3(b.1). After considering the rotational invariance, Eq. (16) is reduced to

$$p_{\alpha'}^{(\lambda+1)}=\sum_{H(1)\ \text{in Fig. 3(b.1)}} w^{\#\#}[H(1)]F_{\alpha'}^{\#}[H(1)], \tag{17}$$

where $w^{\#\#}[H(1)]=\{A\times w[H(1)]\}/\{\Sigma_{H(1)\ \text{of Fig. 3(b.1)}}\, A\times w[H(1)]\}$.

In addition, we can determine the symmetrical invariance in Fig. 3(b.1). For type 2, the two $H(1)$ are symmetrical to each other because of the exchange between LT and RB (denoted as LT$\leftrightarrow$RB). For types 3 and 4.I, the symmetry is due to LT$\leftrightarrow$RT and RT$\leftrightarrow$LB, respectively. For the symmetry of type 5, we find LT$\leftrightarrow$LB, LT$\leftrightarrow$RT, and LT$\leftrightarrow$RB. The number of symmetrical copies for each type is B. We find that $B=1$ (type 1), 2 (type 2), 2 (type 3), 2 (type 4.I), 1 (type 4.II), and 4 (type 5). The $w[H(1)]$ and $F_{\alpha}[H(1)]$ for each symmetrical copy are the same. Therefore, in the calculation of Eq. (16), we can further use only the six kinds of $H(1)$ shown in Fig. 3(b.2). After considering the symmetry, Eq. (16) is reduced to

$$p_{\alpha'}^{(\lambda+1)}=\sum_{H(1)\ \text{in Fig. 3(b.2)}} w^{\#\#\#}[H(1)]F_{\alpha'}^{\#}[H(1)], \tag{18}$$

where $w^{\#\#\#}[H(1)]=\{AB\times w[H(1)]\}/\{\Sigma_{H(1)\ \text{of Fig. 3(b.2)}}\, AB\times w[H(1)]\}$. For $q=3$ or 4, it is more complicated but still straightforward to employ the concepts of rotation and symmetry.

VI. RESULTS OF THE FIXED POINT ANALYSIS

A. Value of the fixed point $(\vec{n}^*,\vec{p}^*)$

The solution of Eq. (16) with the condition $(\vec{n}^{(\lambda+1)},\vec{p}^{(\lambda+1)})=(\vec{n}^{(\lambda)},\vec{p}^{(\lambda)})$ is called the fixed point and is denoted as $(\vec{n}^*,\vec{p}^*)$. To solve $(\vec{n}^*,\vec{p}^*)$, we use an iterative procedure as follows. First, set $(p_1^{(0)},\ldots,p_{q-1}^{(0)},p_q^{(0)})=(0,\ldots,0,1)$. Then, $\vec{n}^{(0)}$ is obtained from Eq. (6). Consecutively, Eqs. (16) and (6) are iterated from $\lambda=0$ to $\lambda=\infty$. Finally, we find that $\vec{p}^{(\infty)}=(0.6060,0.3940)$ for $q=2$, $\vec{p}^{(\infty)}=(0.3835,0.3613,0.2552)$ for $q=3$, and $\vec{p}^{(\infty)}=(0.2317,0.3078,0.2451,0.2154)$ for $q=4$. The fixed point $(\vec{n}^*,\vec{p}^*)$ will correspond to the value of $(\vec{n}^{(\infty)},\vec{p}^{(\infty)})$ under such condition. The values of $\vec{n}^*$ are listed in Table I. The probability of the height being β for the stationary state of the q-state Manna model is numerically performed on a 1000 $\times$1000 square lattice and is also listed in Table I. It was found that the resulting height probabilities of RG are very close to the results obtained from the numerical simulations.

B. Exponent of the toppling number

In Fig. 2, an avalanche leads to the generation of the dynamic λ squares on $\mathcal{L}_\lambda$ where the dynamic two squares [Fig. 2(c)] and three squares [Fig. 2(d)] exist but the dynamic

TABLE I. The values of n_β^* and the corresponding values of the numerical simulations on a 1000×1000 square lattice are listed together.

	n_0^*	n_1^*	n_2^*	n_3^*
$q=2$; RG	0.2827	0.7173		
Simulation	0.2860	0.7140		
$q=3$; RG	0.1363	0.3294	0.5343	
Simulation	0.1425	0.3297	0.5278	
$q=4$; RG	0.0881	0.1884	0.3143	0.4092
Simulation	0.0887	0.1882	0.3068	0.4163

four squares do not exist. According to Pietronero *et al.* [9], the probability of that an avalanche can generate the dynamic λ squares but not the dynamic $(\lambda+1)$ squares is

$$G=\int_{2^\lambda\times2^\lambda}^{2^{(\lambda+1)}\times2^{(\lambda+1)}}D(s)ds\Big/\int_{2^\lambda\times2^\lambda}^{\infty}D(s)ds=1-2^{2(1-\tau)}. \tag{19}$$

On a square lattice $\mathcal{L}_\lambda$, the λ square $i^{(\lambda)}=O$ [marked by △ in Figs. 6(a.1) and 6(b.1)] and the cells containing the λ square O [labeled as I–IV and shown in Figs. 6(a.2) and 6(b.2)] are the objects that we are interested in. Let us consider that at $t=1$ the λ square O is unstable $[h_O(1)=q]$ and that the other λ squares are stable. Then, the λ square O will topple and become a dynamic λ square. In RG language, G is the probability that none of cells I–IV are considered as the dynamic $(\lambda+1)$ square when the evolution triggered by the λ square O stops.

Two ways with probabilities G_a and G_b will contribute to G where $G=G_a+G_b$:

(i) None of the NNs of the λ square O are the dynamic λ square [see Fig. 6(a.1)]. The illustration that none of cells I–IV are considered as the dynamic $(\lambda+1)$ square is shown in Fig. 6(a.2). For $q=2$, the toppling history of Fig. 6(a.1) is shown in Figs. 6(a.3) and 6(a.4). In Fig. 6(a.3), at $t=1$, the λ square O topples through T_{1,d_1} and the d_1 NN of the λ square O possesses a height of 0 where $d_1=$E. This evolution stops at $t=2$ and corresponds to probability

$$G_{a3}=[n_0^{(\lambda)}]\left[\tfrac{1}{4}p_1^{(\lambda)}\right]. \tag{20}$$

In Fig. 6(a.4), at $t=1$, the λ square O topples through T_{2,d_1d_2} for $d_1\neq d_2$ and the d_1 NN and d_2 NN of the λ square O possess a height of 0 where $(d_1,d_2)=$(E,N) or (N,E). This evolution stops at $t=2$ and corresponds to probability

$$G_{a4}=[n_0^{(\lambda)}]^2\left[\tfrac{2}{16}p_2^{(\lambda)}\right]. \tag{21}$$

The total probability of this way is

$$G_a=4G_{a3}+6G_{a4} \tag{22}$$

because the different combinations of d_1 and d_2 are considered.

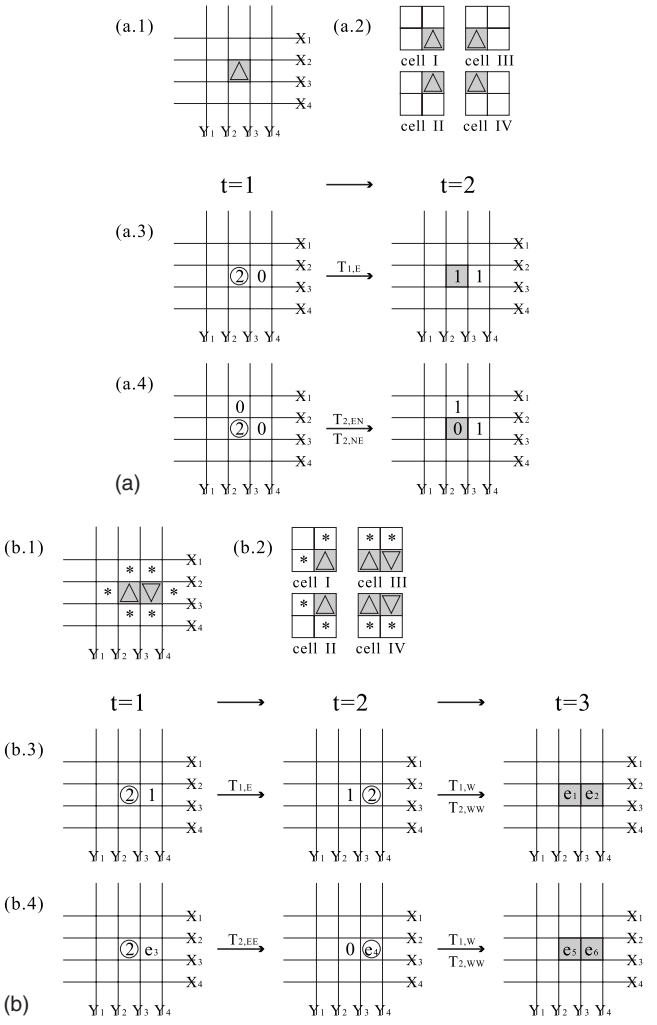

FIG. 6. A square enclosed by lines X_μ, $X_{\mu'}$, Y_ν, and $Y_{\nu'}$ is denoted as $\mathrm{SQ}(X_\mu,X_{\mu'},Y_\nu,Y_{\nu'})$. Cells I–IV are $\mathrm{SQ}(X_1,X_3,Y_1,Y_3)$, $\mathrm{SQ}(X_2,X_4,Y_1,Y_3)$, $\mathrm{SQ}(X_1,X_3,Y_2,Y_4)$, and $\mathrm{SQ}(X_2,X_4,Y_2,Y_4)$, respectively. The λ square O is marked by △. (a.1) Only the λ square O is the dynamic λ square filled in gray. (a.2) The corresponding cells I–IV of (a.1). (a.3) One evolution characterizes the situation of (a.1) where the unstable λ square is marked by ○ and the generated dynamic λ squares are shown in the final height configuration. (a.4) The other evolution characterizes the situation of (a.1). (b.1) Two dynamic λ squares filled in gray exist where the λ square marked by ▽ is a NN of the λ square O. The NNs of the λ squares marked as △ and ▽ are marked by ⋆. (b.2) The corresponding cells I–IV of (b.1). (b.3) and (b.4) Examples of the toppling history of (b.1).

(ii) One NN [marked by ▽ in Fig. 6(b.1)] of the λ square O is also the dynamic λ square. However, all NNs [marked by ⋆ in Fig. 6(b.1)] of △ and ▽ do not receive any λ grain during the evolution triggered by the λ square O. The illustration that none of cells I–IV are considered as the dynamic $(\lambda+1)$ square is shown in Fig. 6(b.2). The reasons are as follows. Both cells I and II contain only one dynamic λ square. Since the spanning rule is not satisfied, cells I and II are not the dynamic $(\lambda+1)$ square. Both cells III and IV contain two dynamic λ squares. However, no λ grain is sent to out of cells III and IV because the λ squares marked as ⋆ do not receive any λ grain. In this case, the forbidding rule is

TABLE II. The RG and simulation values of τ and z.

	RG($q=2$)	RG($q=3$)	RG($q=4$)	Simulation
τ	1.246	1.263	1.271	1.27[a]
z	1.693	1.561	1.506	1.50[a]
$(\tau-1)/z$	0.145	0.169	0.180	0.18[a]

[a]Reference [5].

applied. Therefore, none of cells III and IV are the dynamic $(\lambda+1)$ square. For $q=2$, the toppling history of Fig. 6(b.1) is shown in Figs. 6(b.3) and 6(b.4). In Fig. 6(b.3), at $t=1$, the λ square O topples through $T_{1,\mathrm{E}}$ and the E-NN of the λ square O has a height of 1. This corresponds to probability $[n_1^{(\lambda)}][\frac{1}{4}p_1^{(\lambda)}]$. At $t=2$, the E-NN of the λ square O topples through $T_{1,\mathrm{W}}$ or $T_{2,\mathrm{WW}}$. It corresponds to probability $[\frac{1}{4}p_1^{(\lambda)}+\frac{1}{16}p_2^{(\lambda)}]$. At $t=3$, (e_1,e_2) may be (2,1) or (3,0). Now, the λ square O with $h_O=e_1\geq 2$ is unstable again. According to the freezing rule, every dynamic λ square can topple only once. Thus, this evolution stops at $t=3$ and corresponds to probability

$$G_{b3}=[n_1^{(\lambda)}]\left[\tfrac{1}{4}p_1^{(\lambda)}\right]\left[\tfrac{1}{4}p_1^{(\lambda)}+\tfrac{1}{16}p_2^{(\lambda)}\right]. \tag{23}$$

Similarly, Fig. 6(b.4) characterizes that the λ square O topples through $T_{2,\mathrm{EE}}$ at $t=1$ and its E-NN topples through $T_{1,\mathrm{W}}$ or $T_{2,\mathrm{WW}}$. This evolution also stops at $t=3$ where (e_3,e_4,e_5,e_6) may be (0,2,1,1), (0,2,2,0), (1,3,1,2), or (1,3,2,1). Thus, this evolution corresponds to probability

$$G_{b4}=[n_0^{(\lambda)}+n_1^{(\lambda)}]\left[\tfrac{1}{16}p_2^{(\lambda)}\right]\left[\tfrac{1}{4}p_1^{(\lambda)}+\tfrac{1}{16}p_2^{(\lambda)}\right]. \tag{24}$$

The total probability of this way is

$$G_b=4G_{b3}+4G_{b4} \tag{25}$$

because we consider the different positions of ∇.

For $q>2$, calculating G_a and G_b is still straightforward.

The value of G is calculated by inserting the value of $(\vec{n}^*,\vec{p}^*)$ into $(\vec{n}^{(\lambda)},\vec{p}^{(\lambda)})$. Subsequently, $\tau=1-\ln(1-G)/2\ln(2)$ from Eq. (19). Then, the RG values of $\tau=1.246$ ($G=0.289$ for $q=2$), 1.263 ($G=0.305$ for $q=3$), and 1.271 ($G=0.314$ for $q=4$) are obtained. The RG values listed in Table II are close to the numerical value $\tau=1.27\pm0.01$ [5].

C. Dynamical exponent

Another important physical quantity of the sandpile system is the duration of time t_d which is the number of parallel relaxations on $\mathcal{L}_0$ for an avalanche. The probability distribution of the duration $D(t_d)$ is expected to follow the finite-size scaling form $D(t_d)=t_d^{-\tau_t}\Theta'(t_d/L^z)$, where τ_t is the duration exponent, Θ' is a scaling function, L is the lattice size, and z is the dynamical exponent. Alternatively, if the average duration over all avalanches having the linear size r is $\overline{t_d(r)}$, from [6], we have

$$\overline{t_d(r)}\sim r^z. \tag{26}$$

The simulation values of τ_t and z have been obtained from some extensive simulations, e.g., $\tau_t=1.50\pm0.01$ and $z=1.50\pm0.02$ [5]. Furthermore, a scaling relation [6] between the toppling number s and the duration of time t_d is well verified and is given by

$$(\tau_t-1)/\gamma=(\tau-1)/z. \tag{27}$$

An avalanche is called a $(\lambda+1)$ avalanche if this avalanche leads to the generation of some dynamic λ squares and these generated dynamic λ squares can further evolve into a single dynamic $(\lambda+1)$ square. The sandpile evolution of these generated dynamic λ squares stops at step $t=t_f^{(\lambda)}$. Note that the toppled λ square now is not confined on a 2×2 RG cell and $t_f^{(\lambda)}$ could be larger than 5. Furthermore, the relaxation number of such a $(\lambda+1)$ avalanche counted on $\mathcal{L}_\lambda$ will be $t_f^{(\lambda)}-1$.

Let us assume that a $(\lambda+1)$ avalanche corresponds to linear size $r=2^{\lambda+1}$ and the duration of time $t_d=t_d(2^{\lambda+1})$. Every generated dynamic λ square of a $(\lambda+1)$ avalanche corresponds to linear size $r=2^\lambda$ and the duration of time $t_d=t_d(2^\lambda)$. Then, we have

$$\overline{t_d(2^{\lambda+1})}=\langle t_f^{(\lambda)}-1\rangle\overline{t_d(2^\lambda)}, \tag{28}$$

where $\langle\cdots\rangle$ refers to the average over all $(\lambda+1)$ avalanches. Combining Eqs. (26) and (28), we obtain $\langle t_f^{(\lambda)}-1\rangle=2^z$, i.e., $z=\ln(\langle t_f^{(\lambda)}-1\rangle)/\ln(2)$. From the values of the fixed point $(\vec{n}^*,\vec{p}^*)$ for $q=2$, 3, and 4, we can estimate $\langle t_f^{(\lambda)}-1\rangle$ on $\mathcal{L}_\lambda$ by Monte Carlo simulations. The procedure is as follows:

(1) Randomly assign the height of every λ square on $\mathcal{L}_\lambda$ according to $\vec{n}^{(\lambda)}=\vec{n}^*$.

(2) Add one λ grain to one randomly chosen λ square and then start the sandpile evolution following Eq. (2) where every toppling rule is randomly chosen according to $\vec{p}^{(\lambda)}=\vec{p}^*$. Here, the freezing rule is applied.

(3) When the evolution stops, follow the spanning rule and forbidding rule to check whether this event corresponds to a $(\lambda+1)$ avalanche. Record the value of $t_f^{(\lambda)}-1$ if the evolution is a $(\lambda+1)$ avalanche.

After running the above procedure 5×10^6 times, we obtain $\langle t_f^{(\lambda)}-1\rangle=3.234$ ($q=2$), 2.951 ($q=3$), and 2.840 ($q=4$). Then, the RG values of z are 1.693 ($q=2$), 1.561 ($q=3$), and 1.506 ($q=4$) as listed in Table II. To perform the scaling relation in Eq. (27), the calculation of the values of $(\tau-1)/z$ is also shown in Table II. For τ, z, and $(\tau-1)/z$, we find that the RG values will approach the simulation values as q increases.

D. Summary

This study incorporates the stochastic property into the RG equations of the Manna model. The RG transformation is established by the similarity of topplings observed at different scales. Our proposed RG scheme very efficiently obtains the values of the height probabilities because of the applications of Eq. (13) and four extra transformation rules where the spanning rule maintains the scaling of size, the forbidding rule ensures the dissipation rate at the $(\lambda+1)$th RG stage being zero by dropping that the events do not send any λ grain to out of the RG cell, the freezing rule preserves the driving rate at the $(\lambda+1)$th RG stage being zero and maintains the scaling of the toppling number by setting that every

toppled λ square topples only once, and Eq. (13) maintains the ratio of the number of the received coarse grains to the number of the left coarse grains.

After the calculation of the fixed point $(\vec{n}^*,\vec{p}^*)$ involving only four λ squares of a RG cell, we set $(\vec{n}^{(\lambda)},\vec{p}^{(\lambda)})=(\vec{n}^*,\vec{p}^*)$ and carry out the sandpile evolution on $\mathcal{L}_\lambda$. Through recognizing the formed dynamic λ squares on $\mathcal{L}_\lambda$ as dynamic $(\lambda+1)$ squares or not, we obtain the RG values of τ and z with the help of Eqs. (19) and (28). Since the calculation of τ involves only few λ squares, we count the probability exactly. On the other hand, the calculation of exponents z involves many λ squares. Thus, Monte Carlo method is used to count the probability.

The RG equation shown in Eq. (16) contains only $p_\alpha^{(\lambda)}$, the probability of T_α for $\alpha \geq 1$. Thus, T_0 described by the forbidding rule does not appear in the calculation of n_β^*. However, the effect of T_0 takes place in the calculation of exponents τ and z. For example, the value of $G_b=4G_{b3}+4G_{b4}$ in Eqs. (23) and (24) relates to the probabilities of a $(\lambda+1)$ square possessing toppling rule T_0. From the discussion of the forbidding rule, the probability of T_0 is proportional to the magnitude of dissipation rate. The occurrence of dissipation drives the RG sandpile far from the criticality. This finding provides an explanation for that the values of n_β^* are close to the simulation values but the RG values of τ and z are not. Furthermore, denoting G_b by $G_b(q)$ for the RG calculation of the q-state Manna model, we find $G_b(2)=0.094$, $G_b(3)=0.037$, and $G_b(4)=0.014$. Since the dissipation destroys the criticality, the expression $G_b(2)>G_b(3)>G_b(4)$ provides the reason why the obtained RG values of τ, z, and $(\tau-1)/z$ approach the simulation values as q increases.

ACKNOWLEDGMENT

C.-Y.L. acknowledges the support of the National Science Council of Taiwan, R.O.C. under Grant No. NSC 97-2112-M-194-003-MY2.

[1] P. Bak, C. Tang, and K. Wiesenfeld, Phys. Rev. Lett. **59**, 381 (1987).
[2] H. J. Jensen, *Self-Organized Criticality* (Cambridge University Press, New York, 1998).
[3] S. S. Manna, J. Phys. A **24**, L363 (1991).
[4] A. Chessa, H. E. Stanley, A. Vespignani, and S. Zapperi, Phys. Rev. E **59**, R12 (1999).
[5] A. Chessa, A. Vespignani, and S. Zapperi, Comput. Phys. Commun. **121-122**, 299 (1999).
[6] S. Lübeck, Phys. Rev. E **61**, 204 (2000); Int. J. Mod. Phys. B **18**, 3977 (2004).
[7] D. Dhar, Phys. Rev. Lett. **64**, 1613 (1990); S. N. Majumdar and D. Dhar, Physica A **185**, 129 (1992).
[8] V. B. Priezzhev, J. Stat. Phys. **74**, 955 (1994).
[9] L. Pietronero, A. Vespignani, and S. Zapperi, Phys. Rev. Lett. **72**, 1690 (1994).
[10] E. V. Ivashkevich, Phys. Rev. Lett. **76**, 3368 (1996).
[11] J. Hasty and K. Wiesenfeld, Phys. Rev. Lett. **81**, 1722 (1998).
[12] C.-Y. Lin, A.-C. Cheng, and T.-M. Liaw, Phys. Rev. E **76**, 041114 (2007); A.-C. Cheng, C.-F. Chen, and C.-Y. Lin, Int. J. Mod. Phys. C **19**, 1695 (2008).
[13] C. Tebaldi, M. De Menech, and A. L. Stella, Phys. Rev. Lett. **83**, 3952 (1999).
[14] G. Grinstein, in *Generic Scale Invariance and Self-Organized Criticality in Scale Invariance, Interfaces, and Non-Equilibrium Dynamics*, NATO Advanced Studies Institute, Series B: Physics, edited by A. McKane (Plenum Press, London, 1995), Vol. 344.
[15] D. Sornette, A. Johansen, and I. Dornic, J. Phys. I **5**, 325 (1995).
[16] A. Vespignani, S. Zapperi, and V. Loreto, Phys. Rev. Lett. **77**, 4560 (1996).
[17] C.-Y. Lin, C.-F. Chen, C.-N. Chen, C.-S. Yang, and I.-Min Jiang, Phys. Rev. E **74**, 031304 (2006); C.-F. Chen and C.-Y. Lin, Int. J. Mod. Phys. C **20**, 273 (2009).